VLA Test Memo 143

R. Sramek

October 20, 1983

"VLA Phase Stability at 22 GHz on Baselines of 100m to 3km"

1. Introduction:

Reports from observers tell us that the K band phase stability ranges from very good to hopelessly bad and is often some where in between. This is not very helpful for engineering purposes. Here I will try to make some more quantitative statements about the VLA phase stability based on a series of ten test observing runs at 22 GHz made between 82 Nov and 83 July. This study deliniates the range of expected phase stability and offers some hope that the VLA site may be useful at wavelengths shorter than 1.3cm.

2. Fundamentals:

Consider the visibility phases of an unresolved radio source, measured on a particular baseline, as a time series. The properties of this time series depend on several parameters that we use to restrict the data. Some of the more important parameters are given below.

T_{ave} is the averaging time of the individual phase points. This sets the high frequency cutoff of the power spectrum of the time series.

T_{sam} is the sampling period of the time series.

T_{max} is the longest period observable in the time series, e.g., this may correspond to the length of the observation.

B is the baseline length, i.e., the separation between the antennas; this determines the longest spatial component of the atmosphereic phase distortion that contributes to the time series.

$\Delta(\alpha,\delta)$ is the angular separation in the sky between the radio source and any observed calibrator phase that is subtracted from the time series.

T_{cal} is the characteristic time scale of the calibration.

In addition, the calibration time series may have its own T_{ave} and T_{sam}. The T_{cal} will be determined by the type of interpolation used for the calibration (two-point, boxcar, etc.).

These parameters must be specified whenever we try to compare phase stabilities determined by various observers.

In addition there are many physical characteristics of the atmosphere at the time of observations that determine the phase stability. Since we hope to eventually link the observed phase stability with atmospheric parameters, information such as atmospheric water vapor content, wind velocity, atmospheric lapse rate, barometric pressure, etc. should be given if possible.

2.1 The Allan Variance

The visibility phase time series can be completely characterized by its power spectrum. Howerver, there are serveral disadvantages with using this technique. First, the interferometer phases show a low frequency divergence, or at least the power in the time series is heavily dominated by the longest period sampled. The amplitude of these very long periods, and the amplitude of the sidebands splattered into the higher frequencies, are largely determined by the type of high pass filtering, if any, that the person doing the analysis decides to use. Also, the power spectrum gives too much information about the time series; all we want are a few numbers that chacterize the phase stability which we can correlate with the atmospheric parameters.

In the study of oscillator phase and frequency stability, an Allan variance analysis is often used to circumvent these problems (Blair 1974, Kartaschoff 1978). The Allan variance has a well defined relationship to the phase power spectrum and the phase structure function. It also can be linked to the three-dimensional spatial power spectrum of the atmospheric refractive index (Armstrong and Sramek, 1982, and references cited therin). For a given sampling period, the Allan variance is not very dependent on the total length of the observation or the number of samples. Also, in the limiting case of the two sample variance, this function it is very easy to calculate.

The fractional frequency stability, y(t), is given by

$$y(t) = \delta f(t) / f_o \qquad (1)$$

where $\delta f(t)$ is the deviation at time t of the oscillator frequency from a mean frequency f_o. The two sample Allan variance with zero dead time between frequency measurements is defined as

$$\sigma_y^2(T) = \tfrac{1}{2} \langle (y_{i+1}(T) - y_i(T))^2 \rangle_i \qquad (2)$$

where T is the time over which the fractional frequency observation is made. Writing this in terms of phase,

$$\sigma_y^2(T) = \frac{1}{2} \frac{1}{N} \sum_{i=1}^{N} \left[\frac{(\phi_{i+2} - \phi_{i+1})}{T f_o} - \frac{(\phi_{i+1} - \phi_i)}{T f_o} \right]^2 \qquad (3)$$

$$\tfrac{1}{2} f_o^2 T^2 \sigma_y^2(T) = \frac{1}{N} \sum_{i=1}^{N} \left[\frac{\phi_{i+2} - \phi_i}{2} - \phi_{i+1} \right]^2 \qquad (4)$$

$$\frac{1}{\sqrt{2}} f_o T \sigma_y(T) = \sigma_A(T) \qquad (5)$$

Thus, the rms of the phase after a two-point calibration (denoted by $\sigma_A(T_{sam})$) is just $1/\sqrt{2}$ times the two point Allan variance expressed as a phase. Here the source-calibrator cycle time $T_{cal} = 2*T_{sam}$, and the source calibrator separation is $\Delta(\alpha,\delta) = 0$.

In addition to $\sigma_A(T_{sam})$ derived from the Allan variance, for comparison I've calculated the rms phase (denoted by σ_B) for each time series after first removing a phase drift in time. If this linear phase drift were not removed, the rms values would reflect baseline, UT1, and source position errors in addition to the atmospheric and instrumental drifts that we would like to measure.

3. THE DATA

The ten K-band test observing runs are described in Table I. Typically, each run lasted 4 hours and consisted of 8 minute scans alternating between two sources. The source elevations were typically 40 to 50 degrees. Two pairs of sources were used. On five days the separation of

the sources was 23 degrees, and on 4 days the source separation was 6 degrees. These eight minute scan averages were the primary data sets that were analysed. Parts of the November and June observations and the entire March run consisted of long scans on a single source to study the Allan variance as a function of T_{sam}.

A reference antenna was picked for each observing run that gave a variety of baseline lengths to the other antennas. Typically, twenty to twenty-four antenna pairs were used in the analysis. All the data was taken in either the C or the D configurations, giving baselines of length 60 to 3000m. Since the phase errors are largely antenna based, there is little additional information to be had by considering all possible antenna pairs.

The Allan variance of the phase was calculated for each observing run, for each source on each baseline. Also, the Allan variance was calculated for the difference in phase between the two sources using the normal two point calibration used at the VLA. These Allan variances, expressed as σ_A in degrees of phase at 1.3 cm wavelength, were plotted as a function of baseline length. Fig. 1-3 show typical log-log the plots of σ_A for days with very good, average, and poor phase stability.

The σ_A follow a power law with

$$\sigma_A(T_{sam},B) = \sigma_{A:1km}(T_{sam}) * B^{\alpha} \quad .$$

The slope of the power law, α, and the 1km intercept, $\sigma_{A:1km}$, will be used to characterize the phase stability of each day. The least square fit of this power law is shown on each plot.

In a similar manner, the slope and 1km intercept of σ_B was calculated for each observing run.

4. RESULTS

4.1 Allan Variance Analysis

Table II gives the slope and 1km intercept of $\sigma_A(T_{sam}=16min,B)$ for each of the ten days. Here T_{ave} = 8min. The average values are given at the bottom of the table.

The slope and intercept are also given for the difference in phase of the two sources, i.e., the calibrated phase. Since σ_A is like a self-calibration with $\Delta(\alpha,\delta) = 0$ and $T_{cal} = 2*T_{sam} = 4*T_{ave}$, the additional calibration on the second source with $T_{cal} = T_{sam}$ is not expected to lower the σ_A very much. The observed mean phase of the 1km intercept is only reduced from 18 degrees to 16 degrees by calibration.

4.2 RMS about a Linear Phase Drift

Table III gives the slope and 1km intercept for σ_B, the RMS about a linear phase drift in time. T_{ave} is 8 minutes. For the uncalibrated data T_{cal} is effectively about 4 hours and $\Delta(\alpha,\delta) = 0$. Phase drifts with periods of 8 minutes to 4 hours exist in the time series and therefore σ_B is somewhat larger than σ_A. When the two point calibration is applied T_{cal} is 16 minutes.

The effect of calibration is shown in Figure 4. The 1km intercept of the calibrated and uncalibrated phases are shown separately for the two pairs of sources with $\Delta(\alpha,\delta)$ = 6 degrees and 23 degrees. In general, the calibration only slightly improves the phase r.m.s. and this improvement is not a strong function of angular separation in the 6 to 23 degree range. The average $\sigma_{B:1km}$ is only reduced by 3 degrees when calibration is applied.

4.3 Separating the Instrumental and Atmospheric Phase Errors

Both the instrument and the troposphere contribute to the observed phase errors (the ionospheric contribution is negligible at 1.3cm). The errors due to the troposphere and some of the instrumental contribution are the same in both polarization channels. However, part of the instrumental phase error (e.g. that due to receiver noise) is uncorrelated in the two polarizations and can be estimated by differencing the phases in the two channels. This part of the error is observed to be typically 2 degrees for T_{ave} = 8min. It is rather independent of T_{sam} and is about the same for σ_A and σ_B. Since this instrumental error is much smaller than most of our observed total phase errors, no correction has been applied.

This 2 degree error represents the minimum instrumental contribution. In addition, there is certainly an LO phase error which is not reflected in the phase difference test. This error may increase with baseline length although we don't have a well defined mechanism to produce such an effect.

Therefore, the observed phase errors discussed here represent a total system phase and are an upper limit to the atmospheric contribution. This is encouraging since instruments can conceivably be improved but the atmosphere can't (however, we may be able to monitor it better).

4.4 Average Phase Stability

In order to make some general statement about phase stability, the σ_A measured on all days, on all baselines, and for all sources were binned according to baseline length and averaged. The same was done for the σ_B. The results are summarized in Table IV. Figures 5 and 6 show these

average results for the uncalibrated σ_A with T_{sam} = 16min and 32min. Figure 7 shows the average result for the calibrated σ_B. Since each binned data point represents about 30 observations on ten independent days, the dispersion of the values within each bin can be used to show the range of expected phase stability. The dotted lines represent the least square fit power law to the points one standard deviation above and below the mean line. In general, observations at the VLA have a 68% chance of having an rms phase lieing within the dotted lines.

The results in Table IV show that the 1km intercept is typically 17 degrees and has little dependence on the T_{sam} between 16 min and 32 min. It is not greatly effected by calibration, and is quite independent of the manner of analysis.

5. The Allan Variance as a Function of T_{sam}.

σ_A gives the phase stability on time scale T_{sam}. The total rms phase is equal to

$$\sigma = \sigma_A(T_{sam}) + \sigma_A(2*T_{sam}) + \sigma_A(4*T_{sam}) + \text{(et cet.)}$$

up to $T_{sam} = T_{max}$ (Rogers and Moran, 1981). T_{max} is determined by the duration of the observation or by the time scale on which the cross correlation of the phase errors of the source and calibrator falls to zero. This latter time scale probably increases as the source-calibrator separation increases.

The long observing run on March 26 gives a good analysis of the dependence of σ_A as a function of T_{sam} and T_{ave}. The $\sigma_A(B=1km, T_{sam})$ shown in Figure 8 is fairly flat from T_{sam} = 1 minute to 4 minutes and corresponds to white phase noise. From T_{sam} = 4 minutes to 32 minutes the phase goes as $T_{sam}^{.27}$, slightly steeper than flicker phase noise which goes appproximately as $T_{sam}^{.15}$.

This figure is useful for combining dispersions calculated with different averaging times or sampling times. Based on limited data, the white phase noise and the failure of the noise to reduce as $T_{ave}^{-.5}$ are characteristic of the atmospheric fluctuations for baselines less than a couple kilometers.

6. Phase Stability and Observing Conditions

The on line computers at the VLA apply an atmospheric phase correction based on the surface barometric pressure, temperature, and water vapor content (dew point). These corrections are based on an atmospheric model and they remove the large scale effects of the troposphere. The observed

residual phases reflect the failure of the model, probably on small (ten degree) angular scales.

The parameter $\sigma_{A:1km}$ offers a good measure of the phase stability on a given day. Using T_{sam} = 16 minutes and T_{ave} = 8 minutes as reasonable observing parameters, I've taken the uncalibrated $\sigma_{A:1km}$ shown in Table II, averaged the data for the pair of sources, and compared this quantity with the time/day, the index of refraction due to water vapor, and the wind velocity (Figures 9, 10, and 11 respectively).

Figure 9 indicates that afternoons have poorer phase stability than the rest of the day. Four out of the five runs where $\sigma_{A:1km}$ is greater than 15 degrees occur between 1200 and 1800 MST.

Figure 10 shows no great correlation between water vapor measured at the ground level and the residual phase errors. Either the surface measurements don't reflect the small scale upper atmosphere water vapor content, or water vapor is not the major source of phase error (e.g. we're seeing phase errors due to the dry air contribiution), or the stability of the troposphere is more important than the amount of water vapor.

Figure 11 shows some tendency for the greater phase errors to occur on days with higher wind velocity. Two possible explanations come to mind. First, the phase errors may be due to mechanical motion of the antennas on windy days. Noting that the phase errors get worse on longer baselines, this implies that wind driven antenna movements are the same over a few hundred meters, but at progressivly longer baselines the winds decorrelate and the resulting antenna movements produce baseline errors and thus phase errors. Antenna movements of about a millimeter would explain this effect. The second possible explanation is that wind induced turbulence (in either the wet or the dry air component or both) is causing the observed phase errors. A search for detailed correlation between the wind velocity vector at two antennas (or the antenna tilt) and the phase error could test the first hypothesis.

7. Phase Stability at Shorter Wavelengths

Using T_{sam} = 16 min as typical of a calibrated observing run, Figure 5 allows us to predict how an array of various sizes will perform at shorter wavelength. If you accept one radian as the upper limit of acceptable phase stability for an interferometer, the 14 degree line at 22 GHz in Figuer 5 corresponds to a radian at 88 GHz. For half the time, an array 1 km in size will have phase stability better than this. Longer baselines will have fewer days of acceptable stability.

The phase stability shown in Figure 5 represent the total system phase and is not necessarily a limit impossed by the atmosphere. To the extent

that the phase errors are due to l.o. phase instability or mechanical motion of the antennas the phase stability can conceivably be improved.

Even if the phase errors arise in the atmosphere, water vapor radiometers may give a useful phase correction. And finally, we may be able to predict the time of day or year which give the best phase stability and schedule the shortest wavelength and longest baseline observations at this time.

8. Conclusions

a) The best estimate for the average uncalibrated rms phase, with a time scale of 16 minutes and baselines from 100m to 3000m, is approximately

$$\sigma = (16 \pm 3)\ B(\text{km})^{0.36} \quad \text{degrees}$$

This represents an average of σ_A uncalibrated and σ_B calibrated. The result does not change much by varying the time scale by a factor of two.

b) Since the phase rms given in a) contains a contribution of unknown magnitude from l.o. instabilities, this is an upper limit to the atmospheric phase stability.

c) For baselines of order 1km, σ_A is not a strong function of T_{sam}. Two time ranges are important. For T_{sam} = 1 to 4 minutes we have white phase noise and the phase error is constant. From 4 to 32 minutes, we are in the flicker phase regime, where $\sigma_A = T_{sam}^{.27}$, giving a 20% increase of phase noise for each doubling of T_{sam}. The relevant time scales may change at longer baselines since we would be sampling different size scales in the troposphere.

d) For baselines of order of 1km, T_{cal} = 16 minutes, and with source-calibrator separations of 6 degrees to 23 degrees, two-point calibration does little to improve the phase stability. An average improvement of only three degrees out of twenty can be expected, and this improvement is not a strong function of source-calibrator separation. Only with angular separations of less than a few degrees, where the source/calibrator phase fluctuations are correlated, will rapid switching ($T_{cal} \sim$ 8 minutes, see c) above) be of any help.

e) The phase stability is not worse on days with high dew point, but is worse on days with high wind velocity, usually in the afternoon. This may be due to wind induced turbulence in the atmosphere or to mechanical motion of the antennas.

f) Phase errors of less than one radian can be expected for half the time at baselines up to 1 kilometer at 3mm wavelength.

References:

Armstrong, J.W. and Sramek, R.A., 1982, Radio Science, 17, 1579

Blair, B.E., 1974, "Time and Frequency: Theory and Fundamentals", National Bureau of Standards Monograph 140, U.S. Government Printing Office, Washington. D.C.

Kartaschoff, P., 1978, "Frequency and Time", Academic Press, New York, NY

Rogers, A.E. and Moran, J.M., 1981, I.E.E.E. Trans. on Instrumentaion and Measurement, IM-30, 283

TABLE I

Summary of 22.5 GHz Phase Stability Test Observations

Date	Time (MST) Start	Stop	Sources	Observation
82nov13	0300	1010	0923+392 0917+624	alternate 8min scan; 2.5hr plus single 2.7hr scan
82dec28	0145	0645	0923+392 0917+624	alternate 8min scan; 4.9hr
83jan13	2130	0130	0923+392 0917+624	alternate 8min scan; 3.9hr
83jan15	1330	1630	0224+671 0212+735	alternate 8min scan; 2.9hr
83feb21	0700	1300	0224+671 0212+735	alternate 8min scan; 6.0hr
83mar26	0300	0700	1803+784	single scan; 3.9hr
83apr11	1300	1700	0224+671 0212+735	alternate 8min scan; 3.6hr
83may27	0500	1000	0224+671 0212+735	alternate 8min scan; 5.0hr
83jun04	1220	1620	0923+392 0917+624	alternate 8min scan; 4.0hr
83jul02	1030	1430	0923+392 0917+624	alternate 8min scan; 3.9hr

TABLE II

Summary of results for σ_A at 22.5 GHz

T_{sam} = 16min

Date	Source Declination (degrees)	NO CAL α/	NO CAL $\sigma_{A:1km}$ (degrees)	CAL APPLY α	CAL APPLY $\sigma_{A:1km}$ (degrees)
82nov13	39	.554	14.1	.514	11.1
	62	.712	11.1		
82dec28	39	.619	7.6	.604	7.8
	62	.301	8.4		
83jan13	39	.268	4.7	.431	5.1
	62	.560	9.2		
83jan15	73	.576	21.7	.449	18.4
	67	.801	17.5		
83feb21	73	.525	9.5	.540	9.4
	67	.596	12.7		
83mar26	78	.726	21.6		
83apr11	73	.810	32.0	.782	34.2
	67	.741	28.9		
83may27	73	.619	9.0	.612	9.3
	67	.647	10.1		
83jun04	39	.683	36.0	.658	37.0
	62	.923	59.2		
83jul02	39	.349	9.8	.327	10.5
	62	.611	24.2		
AVERAGE		<.612>	<18.3>	<.546>	<15.9>

NOTE: rms phase(degrees @ 22.5 GHz) = $\sigma_{A:1km} * B^{\alpha}$

where B = baseline length in kilometers

TABLE III

Summary of results for σ_B at 22.5 GHz

Date	Source Declination (degrees)	NO CAL α	NO CAL $\sigma_{B:1km}$ (degrees)	CAL APPLY α	CAL APPLY $\sigma_{B:1km}$ (degrees)
82nov13	39	.274	18.8	.454	10.8
	62	.346	18.8		
82dec28	39	.410	10.1	.396	7.8
	62	.422	9.5		
83jan13	39	.302	16.2	.512	10.1
	62	.363	14.5		
83jan15	73	.613	24.5	.296	17.9
	67	.556	20.0		
83feb21	73	.241	22.6	.534	14.7
	67	.222	23.5		
83mar26	78	.811	24.0		
83apr11	73	.788	34.4	.866	42.6
	67	.689	29.7		
83may27	73	.269	16.8	.669	12.1
	67	.323	18.5		
83jun04	39	.644	43.0	.650	44.9
	62	.666	46.8		
83jul02	39	.421	18.3	.456	17.1
	62	.587	26.4		
AVERAGE		<.471>	<23.0>	<.537>	<19.8>

NOTE: rms phase(degrees @ 22.5 GHz) = $\sigma_{B:1km} * B^{\alpha}$

where B = baseline length in kilometers

TABLE IV
Single Power Law Fit to All Data

Type of Solution	NO CAL		CAL APPLY	
	α	$\sigma_{.1km}$ (degrees)	α	$\sigma_{.1km}$ (degrees)
σ_A (T_{sam}=16min)	.362	14.5	.288	13.1
σ_A (T_{sam}=32min)	.410	17.3	.337	16.4
σ_B	.375	21.5	.351	17.2

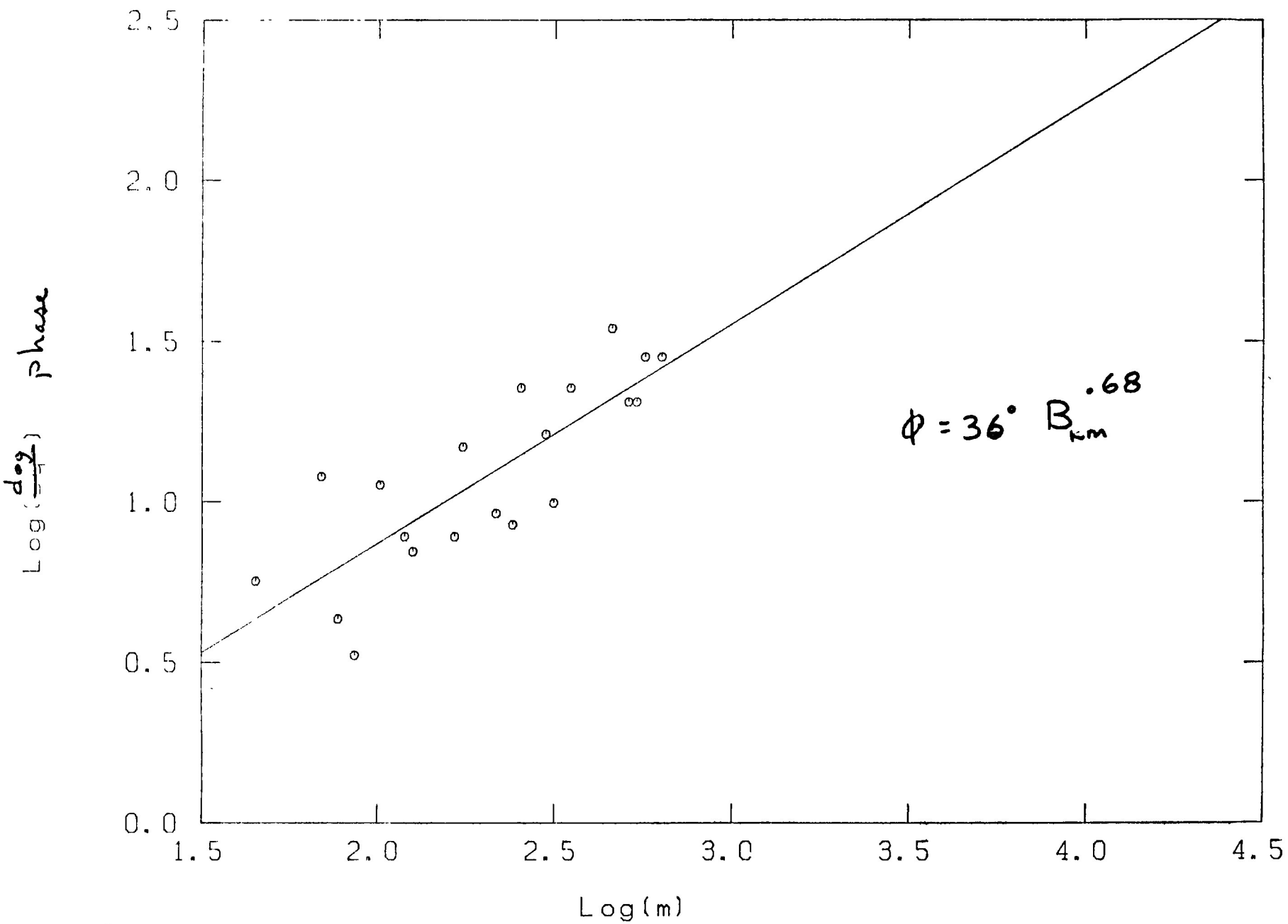
p018a1; cal:none; alt sig2pt; rebin 0
tau = 16 min
2.5
2.0
1.5
1.0
0.5
0.0
1.5
2.0
2.5
3.0
3.5
4.0
4.5
Log(m)
Log(dφ/dt) phase
φ = 36° B_km^.68

Fig. 1

p017a1; cal:none; alt sig2pt; rebin 0
tau = 16 min

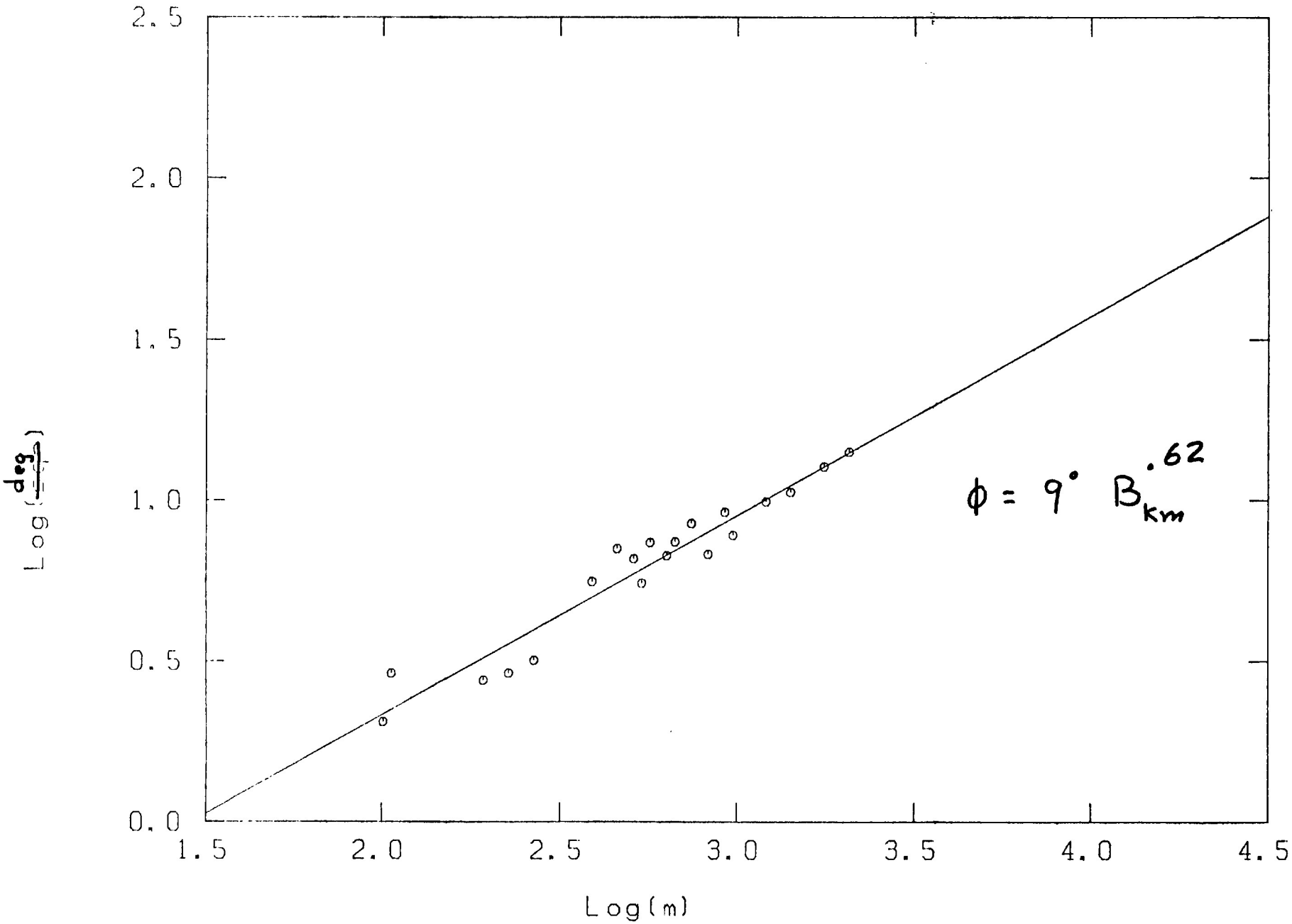

Fig. 2

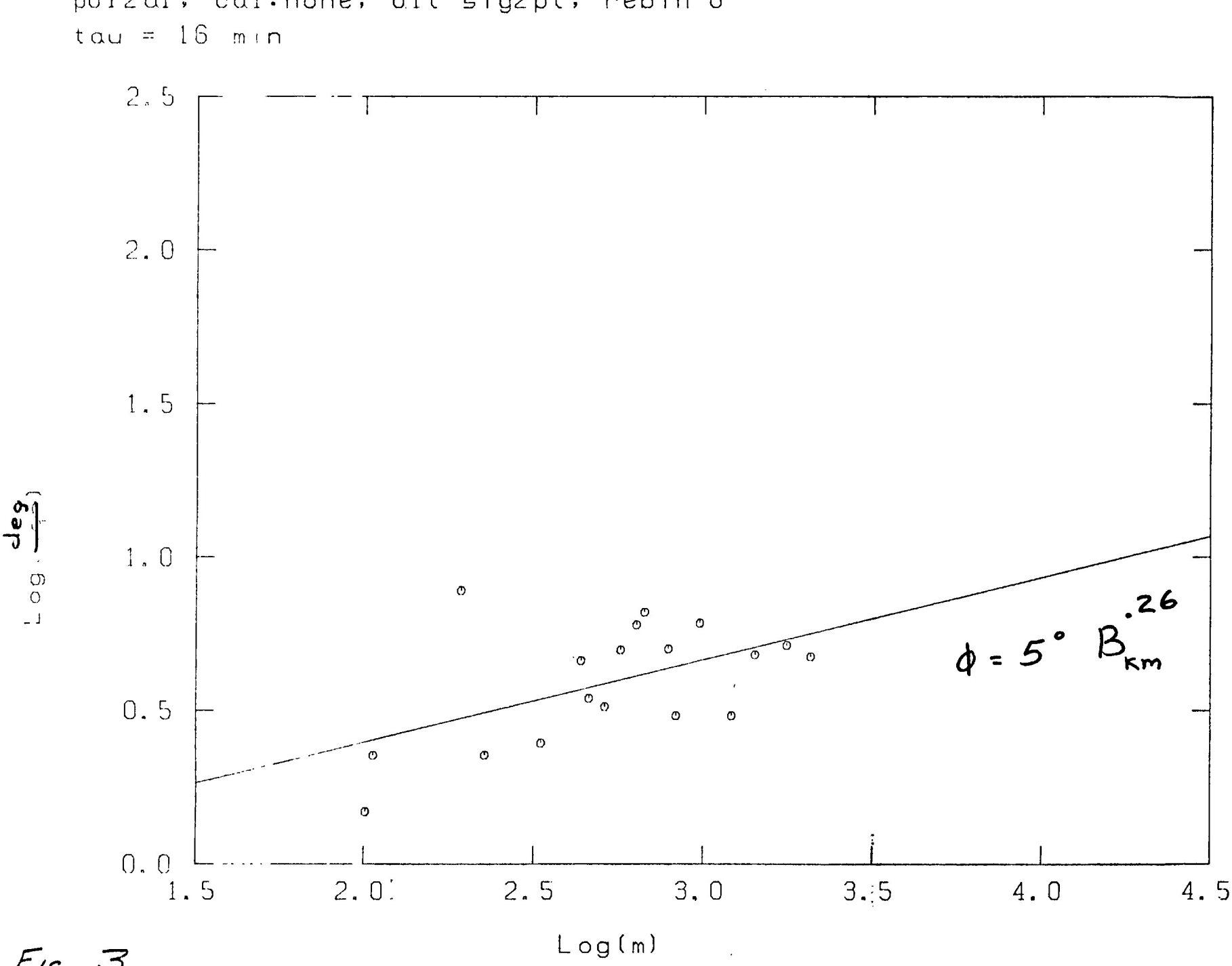
p012a1; cal:none; alt sig2pt; rebin 0
tau = 16 min
2.5
2.0
1.5
1.0
0.5
0.0
1.5
2.0
2.5
3.0
3.5
4.0
4.5
Log(m)
$\phi = 5^\circ B_{km}^{.26}$

Fig. 3

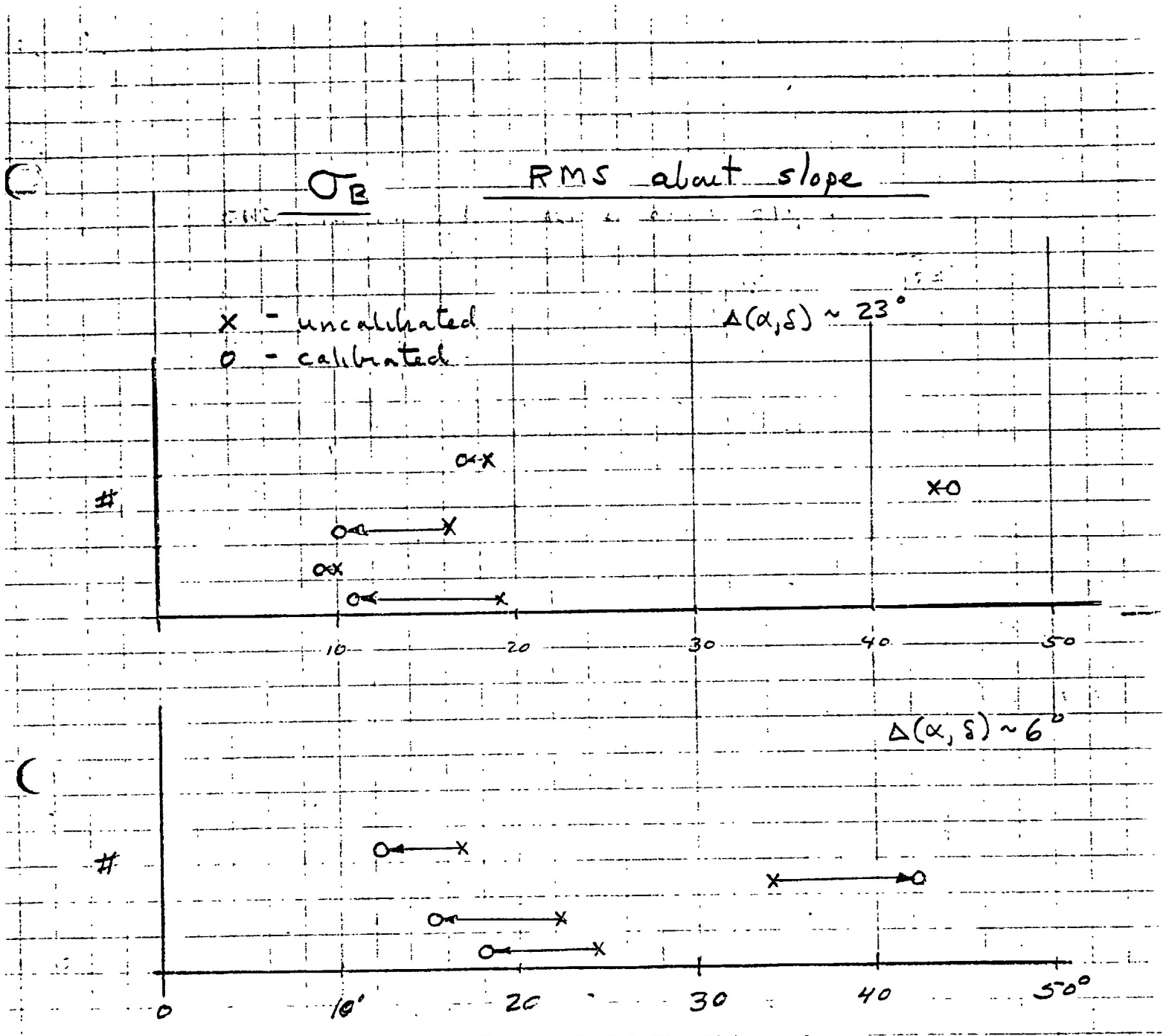

σ_B (1km) (degrees @ 22.5 GHz)

$\tau_{ave.} = 8$ min

$\tau_{max} \sim 4$ hours

$\tau_{CAL} = 16$ min

FIVERAGE σ_E (1km)

	$\Delta(\alpha,\delta)$ 6°	23°
NO CAL	25°	21°
CAL	22°	18°

Fig. 4

ave 18 run*sou; cal:none; sig2pt; rebin 2
tau = 16 min

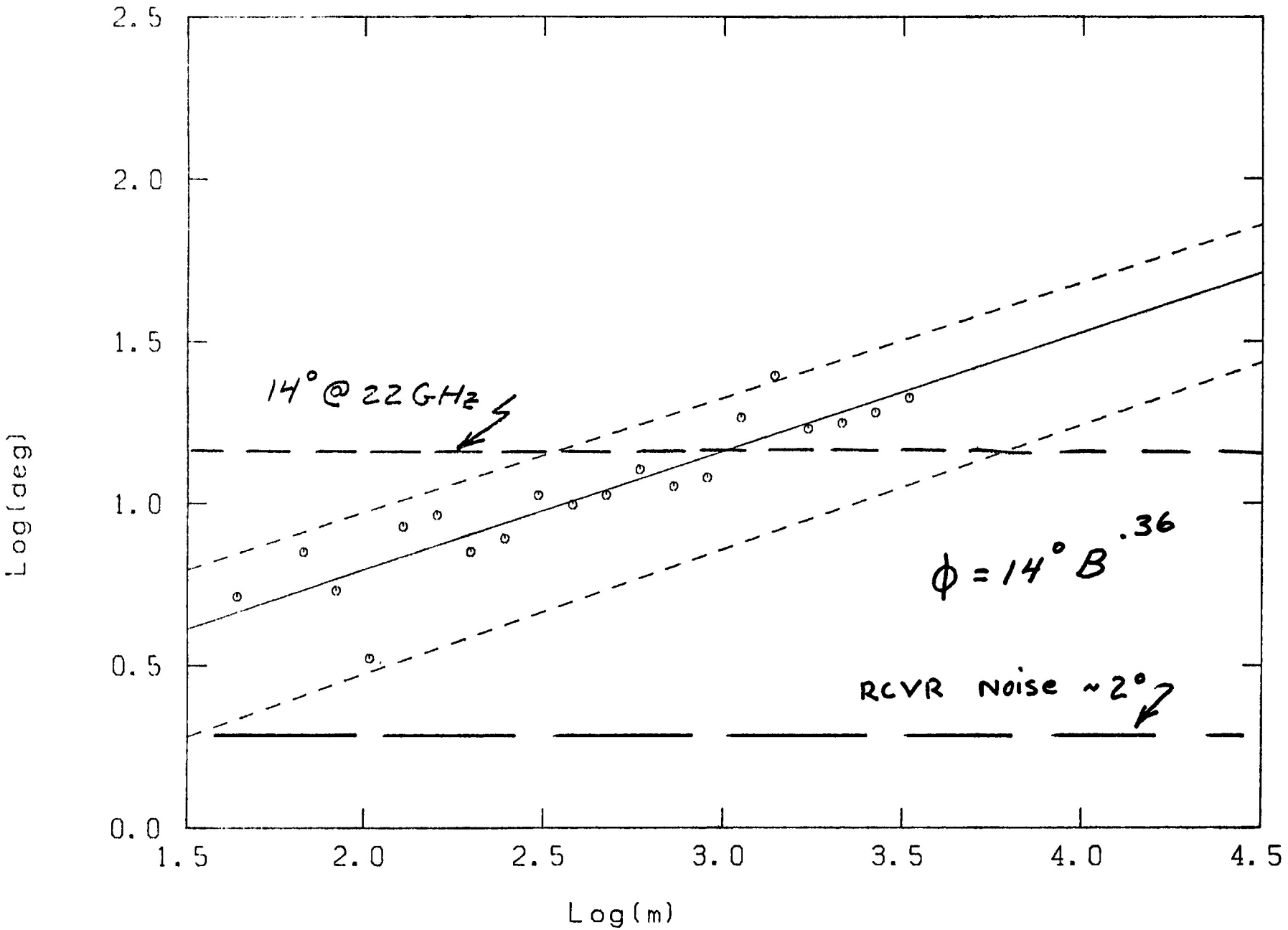

Fig. 5

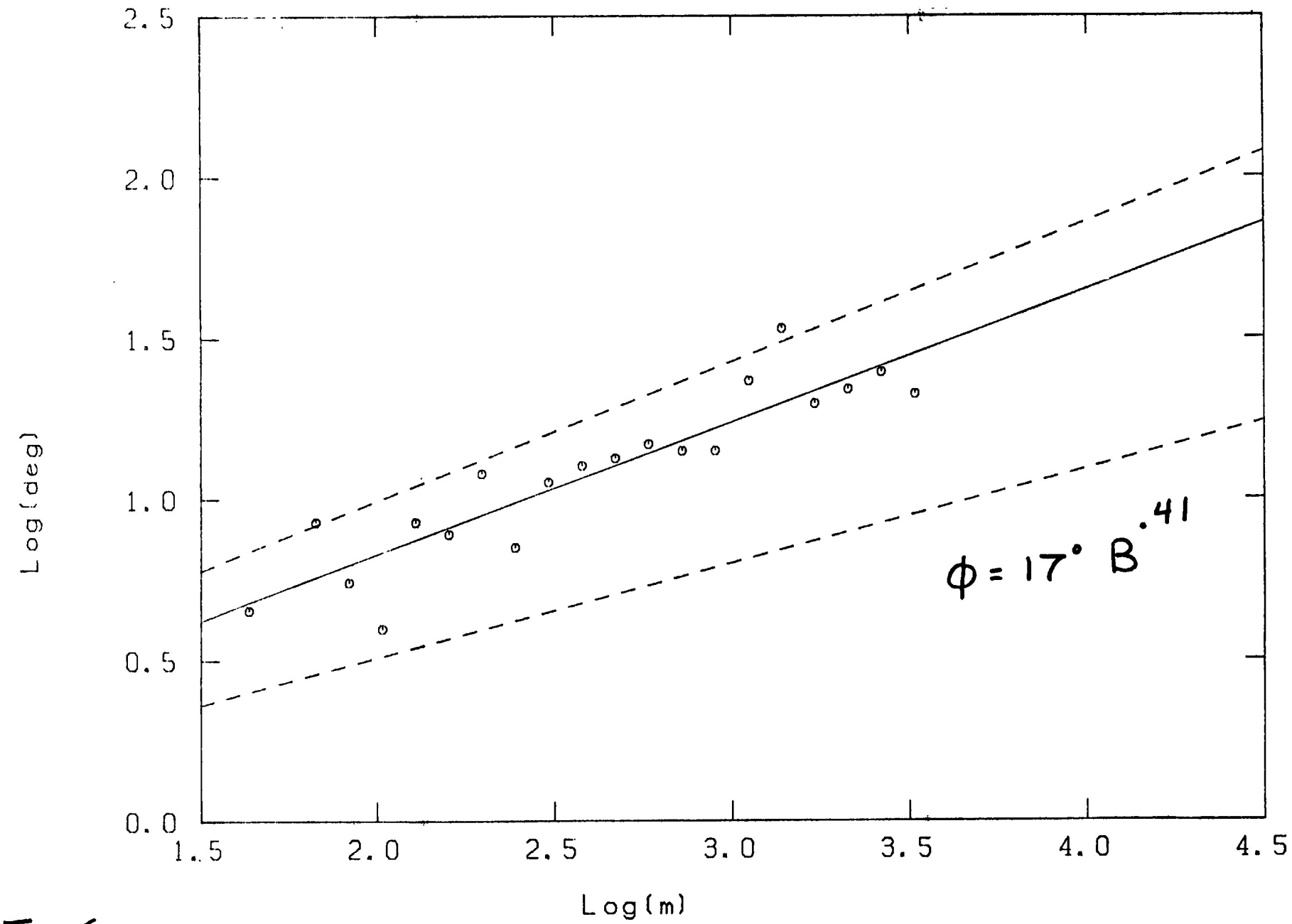
ave .18 run*sou; cal:none; sig2pt; rebin 2
tau = 32 min
2.5
2.0
1.5
1.0
0.5
0.0
Log(deg)
1.5
2.0
2.5
3.0
3.5
4.0
4.5
Log(m)
$\phi = 17^\circ B^{.41}$

Fig. 6

ave 9 run, cal:apply; rms; rebin 2
RMS

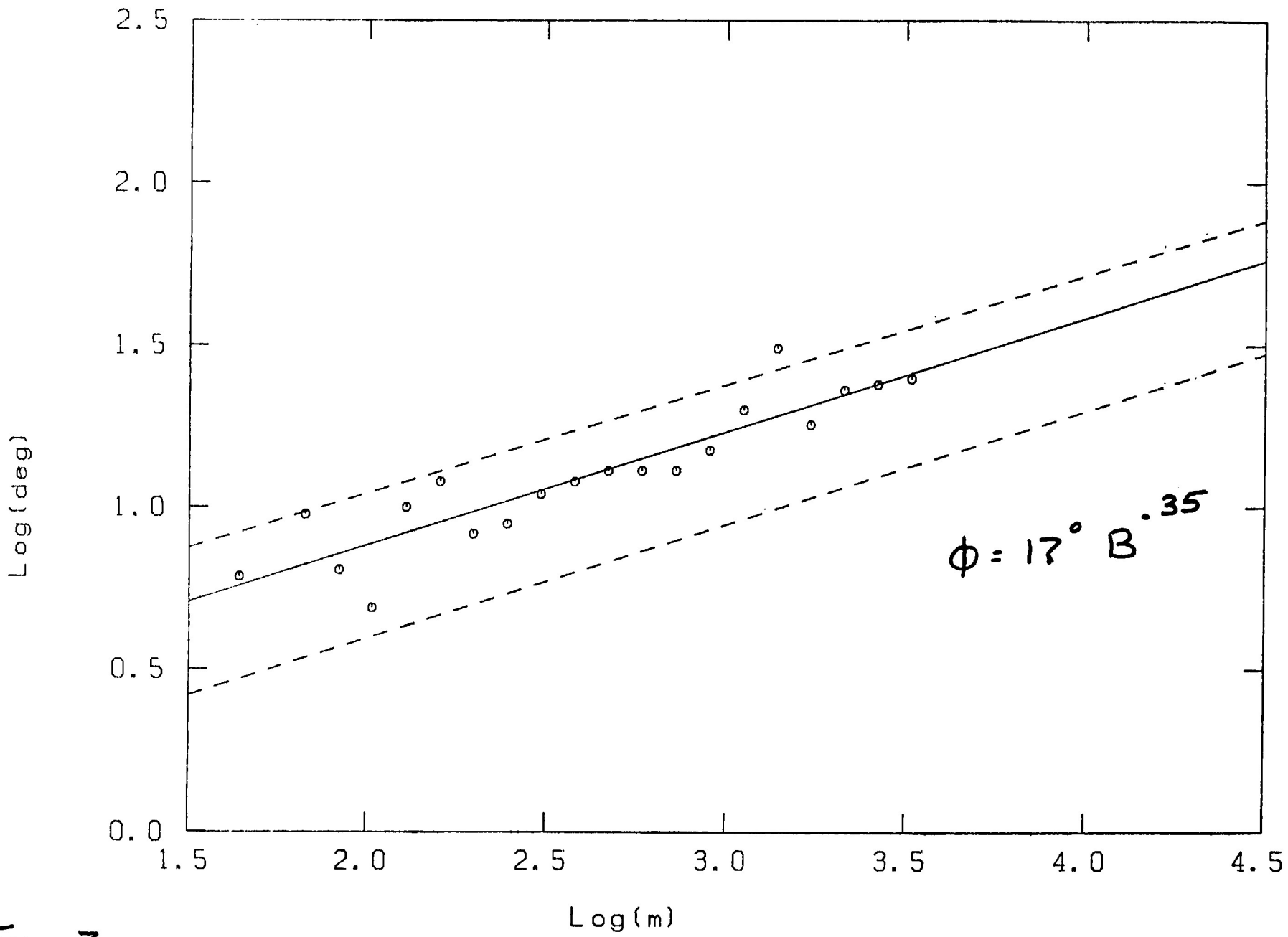

Fig. 7

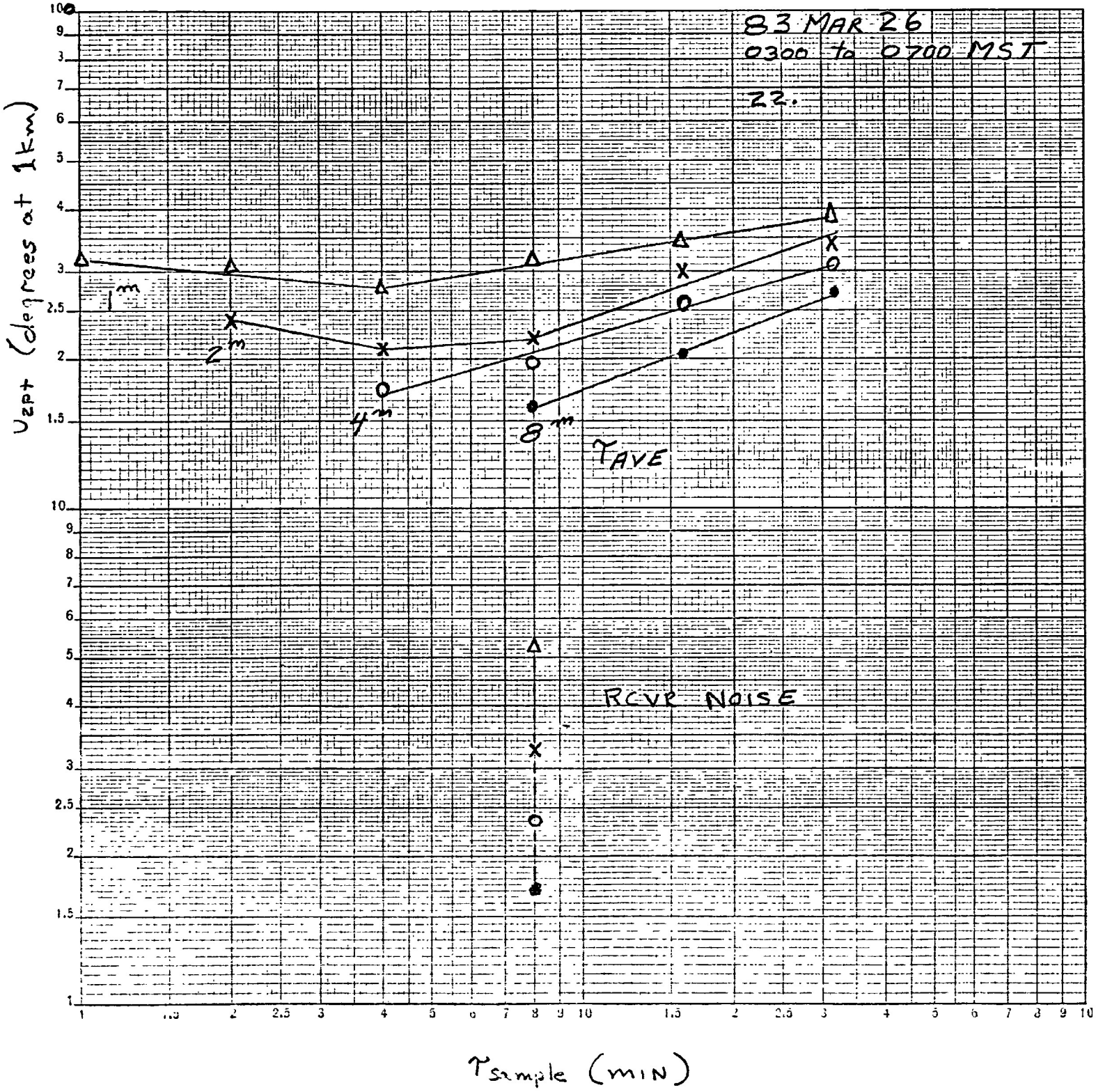
83 MAR 26
0300 to 0700 MST
22.
1m
2m
4m
8m
TAVE
RCVR NOISE
Uzpt (degrees at 1km)
Tsample (MIN)

Fig 8

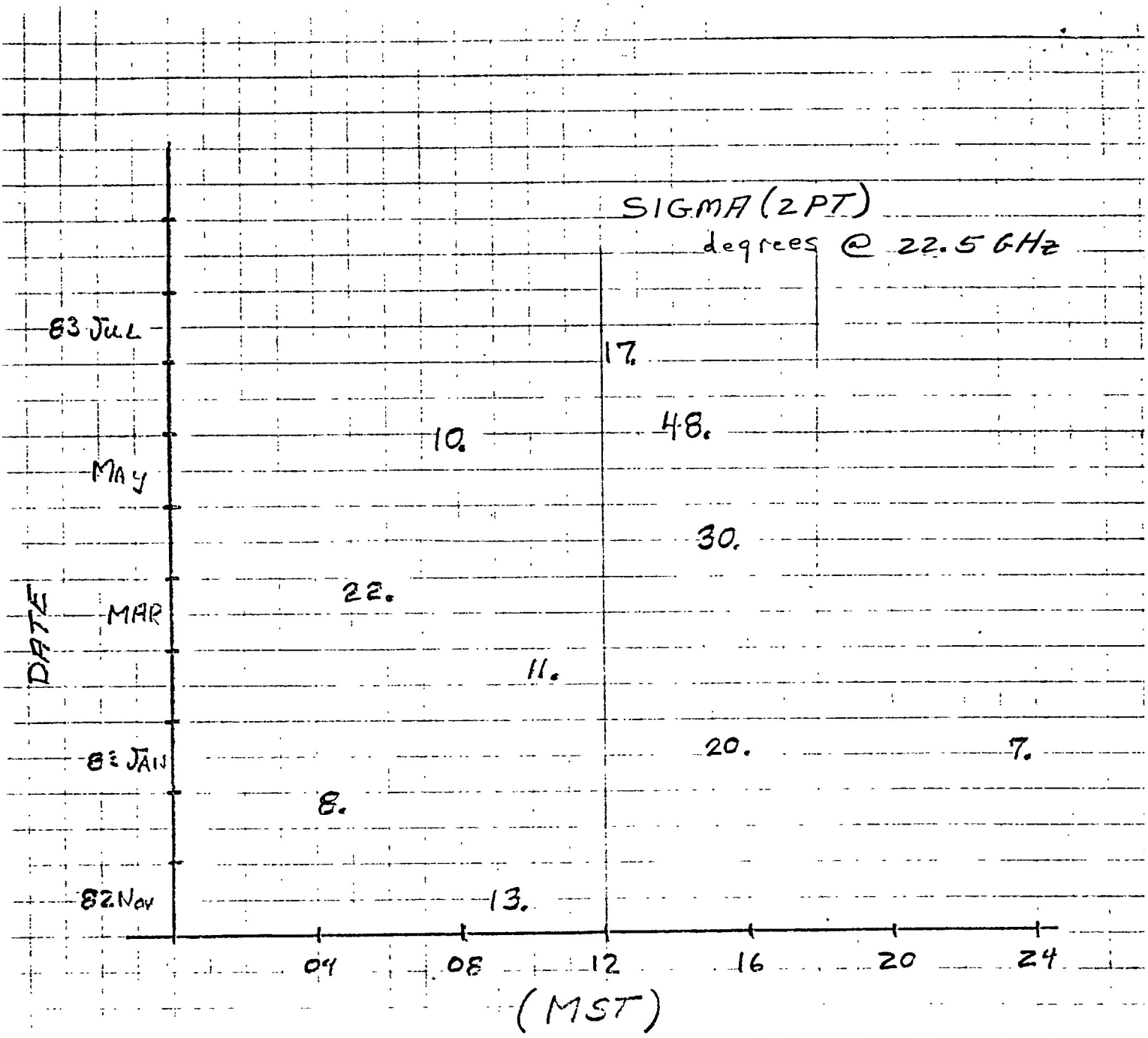

τ_{AVE} = 8 min

τ_{SAM} = 16 min

CAL: NONE

Fig. 9

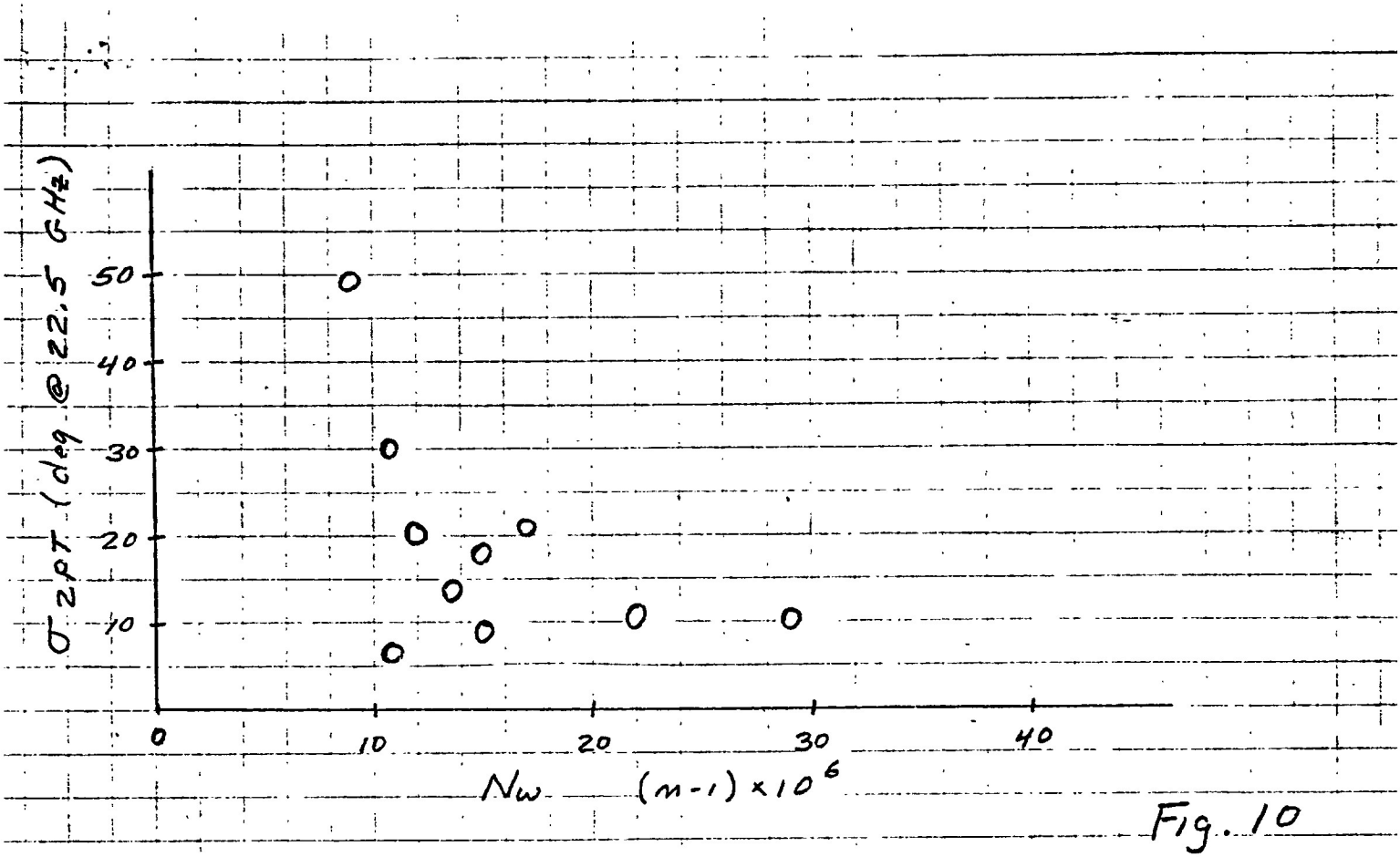
σ 2PT (deg @ 22.5 GHz)
50
40
30
20
10
0
10
20
30
40
Nw (n-1) x 10^6

Fig. 10

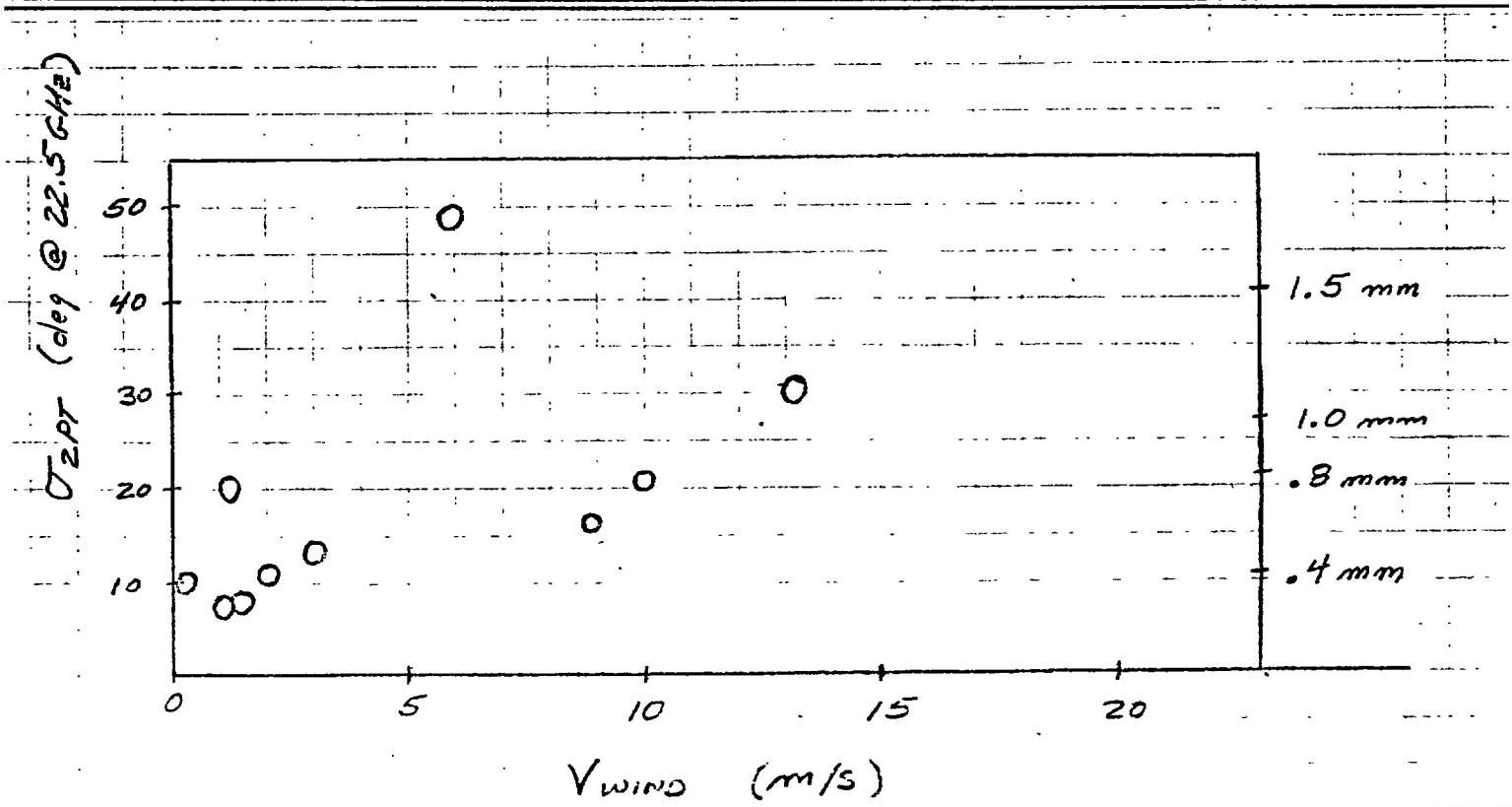
σ 2PT (deg @ 22.5 GHz)
50
40
30
20
10
0
5
10
15
20
V WIND (m/s)
1.5 mm
1.0 mm
.8 mm
.4 mm

Fig. 11